

# Design and Implementation of a Smart Cost-Effective Hearing Aid using Fractional Interpolated Filters\*

TOMSON DEVIS<sup>1</sup> AND MANJU MANUEL  
*Department of Electronics and Communication Engineering  
Rajiv Gandhi Institute of Technology  
Kottayam, 686501 India*  
<sup>1</sup>*APJ Abdul Kalam Technological University  
Kerala, 695016 India*  
*E-mail: tomsondevis@gmail.com; manjum@rit.ac.in*

A reconfigurable hearing aid is capable of adjusting to various impairments without any modification in the hardware. The design and implementation of a reconfigurable filter bank structure of minimal complexity are proposed in this paper for audiogram matching applications. The hearing spectrum is equally decomposed into four regions, and three different schemes are proposed in each region. The Parks McClellan algorithm based prototype filter is fractionally interpolated and various sub-bands are generated for the reconfigurable filter bank. The proposed smart structure can adapt to the optimum scheme by itself based on the hearing characteristics of the impaired person. The structure is tested with different hearing loss scenarios and the matching errors as well as operational delays are found to be within the tolerable limits. The proposed structure requires only 26 multipliers, which saves the hardware by almost 88% with respect to the existing structures. A power and device efficient hardware implementation of the proposed structure is also realized on Kintex7 FPGA board. In addition to the reduced complexity, the proposed structure has the advantage of minimal hardware, which permits the availability of cost-effective hearing aids a reality.

**Keywords:** audiogram matching, filter bank, hearing aid, reconfigurable, fractional interpolation, frequency response masking

## 1. INTRODUCTION

Hearing loss is one of the most common disorders associated with aging in humans. Studies by World Health Organization revealed that about 466 million people in the world suffers from hearing loss [1]. The estimate also states that by 2050, hearing loss has every chance of affecting one among ten people across the world. Some of the major factors resulting in hearing impairment are genetics, certain diseases, noise, drugs, aging *etc.* Hearing loss, if left untreated, has a greater risk of causing other diseases also such as dementia and declining cognitive abilities [2]. The most common type of hearing impairment is sensorineural hearing loss (SNHL) [3]. In SNHL, the sound perception is reduced at any frequency due to the damage of sound sensing hair cells in the inner

---

Received March 13, 2020; revised August 7, 2020; accepted September 14, 2020.  
Communicated by Wen-Liang Hwang.

\* This work was sponsored by the Centre for Engineering Research and Development (CERD) of APJ Abdul Kalam Technological University, Kerala, India (Grant No: KTU/A/199/2016).

ear. Another type of hearing loss that affects both ears simultaneously is presbycusis [4]. Presbycusis occurs naturally on high frequency sounds due to the diminishing performance of the hair cells in the ear due to aging. Since presbycusis occurs gradually, people may not be able to recognize their diminishing hearing ability [5].

Hearing aid is an assistive device used by the hearing impaired people to make sounds louder. Among the various type of hearing aids available, digital hearing aids are the most popular as it can perform various signal processing operations on the incoming signal effectively to enhance the overall perception of sound [6]. Even though digital hearing aids are able to perform various functions such as speech enhancement, noise reduction and feedback cancellation, auditory compensation is its basic function. Most of the hearing aids are designed and fitted to correct SNHL. Even though a large number of people suffers from hearing disorders which can be corrected by the use of hearing aids, its current production is able to meet only less than 10% of the global need.

In the hearing aid designs reported in previous works with good matching performance, the complexity is high, making the situation worse. With increase in complexity, the hearing aid becomes hardware-rich making it expensive, resulting in an unaffordable hearing aid for the public. Hence, most of the problems associated with hearing remain unresolved, which points out to the urgent need for development of affordable hearing aids. A good reduction in complexity is achieved in the proposed work by reducing the number of multipliers, which is the most power consuming element in the hardware. The proposed low complexity design aids in reducing the complex hardware required for the manufacture of hearing aids, thereby reducing the cost of production which ultimately results in making the hearing aid cost-effective.

Yet another promising feature of the proposed work is the reconfigurability introduced, which permits adaptation to various hearing impairments. A reconfigurable hearing aid can be used for various types of hearing impairments without any alteration in the device hardware. But the existing reconfigurable hearing aids require trial and error methods to fix the proper bands in various frequencies which is a very time consuming and tiresome process [7, 8]. This is completely eliminated by the use of a smart scheme selection method proposed in this paper.

The remaining sections of this paper are organized as follows. The different auditory compensation techniques are presented in Section 2. The design and hardware implementation of the proposed reconfigurable hearing aid are explained in Section 3. The performance analysis of the proposed structure is presented in Section 4 and the conclusions are made in Section 5.

## 2. BACKGROUND

Auditory compensation is the process of adjusting the gains of sub-filters of the filter bank in a digital hearing aid, based on the hearing profile [2]. Selective amplification procedure in digital hearing aids was addressed with uniform filter banks initially, but the matching performance obtained was just moderate. As the hearing response is logarithmic, the use of non-uniform filter banks would be more beneficial for auditory compensation. Several methods were employed by researchers to generate non-uniform filter banks from the prototype filter. One among them is the ANSI S1.11 filter bank

(ANSI) using 18 numbers of 1/3 octave filters, which gives the best matching. But the group delay and device complexity of this fixed filter bank method are very high compared with other techniques [9]. Even though an unstrained version of this method called the Quasi-ANSI S1.11 filter bank has less delay, it has increased complexity [10]. Frequency response masking (FRM) technique is utilized for the non-uniform filter bank generation in [11, 12]. This method gives sharp narrow band digital filters from less complex sub-filters. But the group delay of this method is very high compared with other techniques. The prototype filter is cosine modulated to get an array of uniform filters in [7]. Non-uniform cosine modulated filter banks (CMFB) are realized by adjacent band merging and transition filter approaches. But the device complexity of this technique is high.

A variable bandwidth (VBW) filter using sampling rate conversion technique for generating the non-uniform sub-bands of the prototype filter is presented in [13]. The reconfigurable hearing aid using VBW filter [14] requires very complex hardware for implementation. VBW filter using farrow structure is introduced in [15], which gives good matching results with lower delay, but has increased hardware complexity. Non-uniform filter banks are achieved by modified discrete Fourier transform (MDFT) method is presented in [8], which requires complex hardware for realization. Non-uniform filter banks are designed using a fractional interpolated (FI) filters in [16] and [17], which employs a combination of decimation and interpolation operations for sub-band generation. This method has moderate complexity, but the delay of this method exceeds the accepted range when compensating audiograms with sharp variations. A two-level sound wave decomposition structure based on FI is presented in [18]. This method gives better compensation in addition to the use of less hardware. An interpolated finite impulse response filter with moderate complexity is used to generate a 17-band fixed filter bank [19]. The smart reconfigurable filter bank structure proposed in this paper features auto reconfiguring capability and requires only 26 multipliers which is better than other existing techniques for implementation.

## 2.1 Finite Impulse Response Filter

The increased stability, symmetric coefficients, and the linear phase response of the finite impulse response (FIR) filter makes it best suited for audio processing applications [20]. The non-recursive nature of the FIR filter can be beneficially used in hearing aids. The lowest order FIR filter with equi-ripples in passband and stopband is realized by the Advanced Remez Exchange algorithm or Parks-McClellan algorithm [21]. The Kaiser formula based Parks-McClellan algorithm for a filter of order  $N$  is given by

$$N = \frac{-20 \log_{10}(\sqrt{\delta_p \delta_s}) - 13}{14.6(\omega_s - \omega_p)/2\pi} \quad (1)$$

where  $\delta_p$  and  $\delta_s$  are the maximum permitted ripples in the passband and stopband respectively, and  $\omega_p$  and  $\omega_s$  are the passband and stopband edge frequencies. This design requires  $N$  adders and  $\lceil \frac{N+1}{2} \rceil$  multipliers for the realization of the filter.

Interpolation and decimation operations are used to adjust the passband width of the prototype filter. In multirate signal processing, the interpolation operation increases the sampling rate by a factor  $L$ , and the decimation operation decreases the sampling rate by

a factor  $D$  [22]. In the time domain, the interpolation process will introduce  $L - 1$  null samples in between each original sample, and the decimation process groups every  $D^{\text{th}}$  samples [23]. In the frequency domain, the interpolation and decimation processes are represented as  $H(z^L)$  and  $H(z^{1/D})$ . Fractional interpolation is a combination of these two operations and described as  $H(z^{L/D})$ . In the fractional interpolated filter  $H(z^{L/D})$ , every  $D^{\text{th}}$  coefficients of the prototype filter are grouped together and  $(L - 1)$  zeros are inserted between the coefficients.

### 3. PROPOSED METHODOLOGY

The prototype low-pass filter,  $H(z)$  has cut-off frequency at 2kHz and bandwidth  $\pi/4$ . The sampling frequency,  $f_s$  of 16kHz, passband ripple,  $\delta_p$  of 0.05dB, and stopband attenuation,  $\delta_s$  of 50dB are selected as the specifications of  $H(z)$ .  $H(z)$  is realized by the minimax approximation principle using the Parks McClellan algorithm [21]. This achieves a stable FIR filter of optimized order with equi-ripple passband and stopband based on the given specifications. The magnitude response of the proposed prototype filter,  $H(z)$  is represented in Fig. 1 (a).

The passband of the prototype filter,  $H(z)$  of order  $N$  is symmetrically shifted using low pass to high pass transformation. The resultant complementary filter,  $H_c(z)$  is represented in Eq. (2(a)). Fractional interpolations [24] are performed on the prototype filter,  $H(z)$  for generating more number of sub-filters with desirable bandwidth. The fractional interpolated filters are represented as  $H(z^{L/D})$  with an interpolation factor  $L$ , is selected as 1, 4, 8 and the decimation factor  $D$ , is selected as 2.  $H(z^{1/2})$ ,  $H(z^{4/2})$ , and  $H(z^{8/2})$  are generated and its complementary pairs are created using Eqs. (2(b)-(d)). The parameter  $\Delta$  in the equations represents the half length of the corresponding filter. The magnitude responses of the fractional interpolated filters and its complementary pairs are illustrated in Fig. 1 (a) and (b), respectively.

$$\begin{aligned}
 H_c(z) &= z^{-(N-1)/2} - H(z) & \text{(a)} \\
 H_c(z^{1/2}) &= z^{-\Delta} - H(z^{1/2}) & \text{(b)} \\
 H_c(z^{4/2}) &= z^{-\Delta} - H(z^{4/2}) & \text{(c)} \\
 H_c(z^{8/2}) &= z^{-\Delta} - H(z^{8/2}) & \text{(d)}
 \end{aligned} \tag{2}$$

In the proposed reconfigurable auditory compensation method, the audio spectrum is equally divided into four regions of bandwidth  $\pi/4$ , and three different schemes are suggested in each region. Table 1 gives the number of sub-bands and their bandwidth in different regions according to various schemes. A suitable combination of  $H(z)$ ,  $H(z^{1/2})$ ,  $H_c(z)$ , and  $H_c(z^{1/2})$  are used to produce the 4-band uniform filter bank with a bandwidth of  $\pi/4$ . Since the filter bank have only one band per region, these bands itself are used as the masking filters for different regions in higher schemes.  $H(z^{4/2})$  and  $H_c(z^{4/2})$  are used along with the above filters to create the 8-band uniform filter bank with a bandwidth of  $\pi/8$ , which have two bands in each region.  $H(z^{8/2})$  and  $H_c(z^{8/2})$  are employed in addition to the above filters to generate the 16-band uniform filter bank with a bandwidth of  $\pi/16$ , which have four bands in each region. The transfer functions of the sub-bands

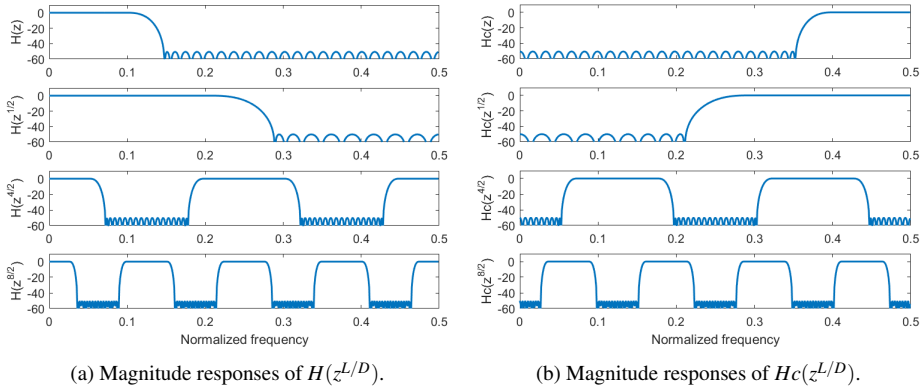


Fig. 1. Magnitude responses of the prototype and fractional interpolated filters.

of different schemes in various regions are listed in Table 2. The magnitude responses of the bands in different schemes in each region are shown in Fig. 2. The sub-bands are represented in general as ' $B_{ijk}$ ', where ' $i$ ' corresponds to the scheme, ' $j$ ' represents the region, and ' $k$ ' stands for the band number. For example, ' $B_{231}$ ' defines the first band in the third region, when scheme 2 is used.

**Table 1. Number of bands and bandwidth distributions in different schemes.**

Scheme	Number of bands				Bandwidth
	Region 1	Region 2	Region 3	Region 4	
Scheme 1	1	1	1	1	$\pi/4$
Scheme 2	2	2	2	2	$\pi/8$
Scheme 3	4	4	4	4	$\pi/16$

### 3.1 Selection of Optimal Transition Width

The complexity of the proposed system depends on the order of  $H(z)$ . The order of  $H(z)$  is inversely proportional to the transition width between the passband and stopband. Besides, the transition width of the generated sub-bands in various schemes also depends on the transition width of  $H(z)$ . The optimum selection of the transition width of  $H(z)$  is estimated, based on the matching error calculation of the audiogram of the right ear in Fig. 6 (a). The matching error is calculated with normalized transition widths varying from 0.07 to 0.11 and listed in Table 3. The order of the prototype filter,  $H(z)$  is computed using the Parks-McClellan algorithm with passband and stopband cutoff frequencies  $w_p$  and  $w_s$ . It is apparent from Table 3 that the proposed system provides a minimum matching error for the transition bandwidth of 0.105. A further increase in transition width causes an increment in the matching error due to the enhanced overlapping of adjacent sub-bands. Hence, the order of the prototype filter is selected as 51, and only 26 multipliers are required for implementation.

### 3.2 Delay Analysis of the Proposed Method

Hearing-impaired people use different techniques to improve their hearing perception. Most of them carefully watch the lip movements of the speaker in addition to

**Table 2. Transfer functions of the sub-bands in different schemes.**

Scheme 1			Scheme 2			Scheme 3		
Band	Region	Transfer function	Band	Region	Transfer function	Band	Region	Transfer function
$B_{111}$	1	$H(z)$	$B_{211}$	1	$H(z^{4/2})$	$B_{311}$	1	$H(z^{8/2})H(z^{4/2})$
$B_{121}$	2	$H(z^{1/2}) - H(z)$	$B_{212}$	1	$H_c(z^{4/2})$	$B_{312}$	1	$H_c(z^{8/2})H(z^{4/2})$
$B_{131}$	3	$H_c(z^{1/2}) - H_c(z)$	$B_{221}$	2	$H_c(z^{4/2})$	$B_{313}$	1	$H_c(z^{8/2})H_c(z^{4/2})$
$B_{141}$	4	$H_c(z)$	$B_{222}$	2	$H(z^{4/2})$	$B_{314}$	1	$H(z^{8/2})H_c(z^{4/2})$
			$B_{231}$	3	$H(z^{4/2})$	$B_{321}$	2	$H(z^{8/2})H_c(z^{4/2})$
			$B_{232}$	3	$H_c(z^{4/2})$	$B_{322}$	2	$H_c(z^{8/2})H_c(z^{4/2})$
			$B_{241}$	4	$H_c(z^{4/2})$	$B_{323}$	2	$H_c(z^{8/2})H(z^{4/2})$
			$B_{242}$	4	$H(z^{4/2})$	$B_{324}$	2	$H(z^{8/2})H(z^{4/2})$
						$B_{331}$	3	$H(z^{8/2})H(z^{4/2})$
						$B_{332}$	3	$H_c(z^{8/2})H(z^{4/2})$
						$B_{333}$	3	$H_c(z^{8/2})H_c(z^{4/2})$
						$B_{334}$	3	$H(z^{8/2})H_c(z^{4/2})$
						$B_{341}$	4	$H(z^{8/2})H_c(z^{4/2})$
						$B_{342}$	4	$H_c(z^{8/2})H_c(z^{4/2})$
						$B_{343}$	4	$H_c(z^{8/2})H(z^{4/2})$
						$B_{344}$	4	$H(z^{8/2})H(z^{4/2})$

employing hearing aids. To ensure that the speaker's voice reproduced in the hearing aid is synchronized with the lip movements of the speaker, the maximum delay of the audio filters is limited to 20ms in digital hearing aids [25]. The operational delay of a fractional interpolated FIR filter with order  $N$  is given by

$$T = \frac{NL}{2Df_s} \quad (3)$$

where  $L$  and  $D$  are the interpolation and decimation factors,  $f_s$  is the sampling frequency respectively. In the proposed structure, the order of the prototype filter is 51, and the sampling frequency is 16kHz. The delays of  $H(z)$  and  $H(z^{1/2})$  are 1.59ms and 0.79ms and of  $H(z^{4/2})$  and  $H(z^{8/2})$  are 3.18ms and 6.36ms respectively. Since various schemes uses different filters in cascade manner, the cumulative delay is taken for the corresponding scheme. The group delays associated with different schemes of the proposed method are listed in Table 4.

### 3.3 The Smart Scheme Selection Procedure

The selection of optimum scheme in all other existing reconfigurable hearing aids are based on trial and error method. Initially, lower schemes are selected in all regions, and the matching errors are calculated. When the matching error of any region is beyond the acceptable limit of  $\pm 3dB$ , the next higher scheme is selected in that region and the process is repeated until the errors in all regions are within the limit. In the proposed method, an automated selection of the schemes are employed with the variations in hearing profile shown in the audiogram. An audiogram indicates the softest sounds that can be heard by an impaired person at different octave frequencies, *i.e.*, at 250Hz, 500Hz, 1kHz, 2kHz,

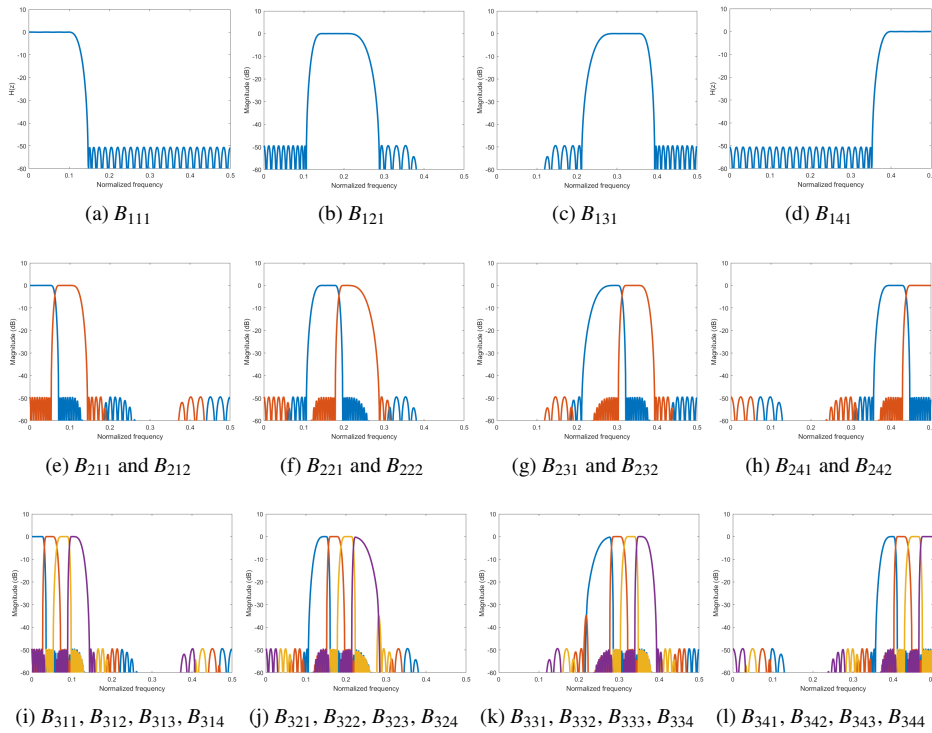


Fig. 2. Sub-bands of scheme 1, scheme 2, and scheme 3 in different regions.

4kHz, and 8kHz [26]. In the audiogram, the frequencies in hertz (Hz) are shown on X-axis, and the responses of the ear in decibels (dB) are shown on Y-axis. The response of the right and left ears are represented by the symbol ‘O’ and symbol ‘X’ respectively.

An audiogram consists of six hearing threshold values at different octaves. The deviations in hearing levels between two adjacent octaves are calculated and used as the selection criterion for various schemes. The audiogram matrix,  $a_i$ , has six different hearing threshold values, and the corresponding slope matrix,  $d_i = a_{i+1} - a_i$  have five elements. Since there are three slope values in the first region ( $0 - \pi/4$ ), the rising or falling trend of hearing is estimated by taking the combinations of these slopes. The hearing variation,  $V_k$  in any region  $k$  is calculated from the slope values,  $d_i$  as listed in Table 5. These variations are used to estimate the optimum scheme in different regions. When the upper threshold of  $V_k$  is 5dB, scheme 1 is selected in region  $k$ . Similarly, an upper threshold of 15dB and 30dB in any region confirms the scheme 2 and scheme 3 in the corresponding region.

### 3.4 Structure of the Proposed Reconfigurable Filter Bank

The structure of the proposed reconfigurable filter bank is shown in Fig. 3. In every filter, the low pass output of the filter is represented as ‘o’, and its complementary output is indicated by ‘c’. A 3-bit control signal,  $S = S_1S_2S_3$ , is used to enable various stages of the structure and hence, to select the different schemes in respective regions. A bit ‘1’

**Table 3. Selection of optimal transition width.**

Transition width	passband edge, $w_p$	stopband edge, $w_s$	Filter order	Number of multipliers	Maximum matching error (dB)
0.07	0.215	0.285	79	40	3.47
0.075	0.2125	0.2875	75	38	3.34
0.08	0.21	0.29	69	35	3.18
0.085	0.2075	0.2925	65	33	2.95
0.09	0.205	0.295	63	32	2.72
0.095	0.2025	0.2975	59	30	2.54
0.1	0.20	0.30	55	28	2.38
<b>0.105</b>	<b>0.1975</b>	<b>0.3025</b>	<b>51</b>	<b>26</b>	<b>2.23</b>
0.11	0.195	0.305	49	25	2.41

**Table 4. Delays associated with different schemes.**

Scheme	$S_1S_2S_3$	Filters used	Delay
Scheme 1	001	$H(z^{1/2}), H(z)$	2.38ms
Scheme 2	010	$H(z^{4/2}), H(z^{1/2}), H(z)$	5.56ms
Scheme 3	100	$H(z^{8/2}), H(z^{4/2}), H(z^{1/2}), H(z)$	11.92ms

in the control signal will close the normally opened switch. Initially, the control switch status ‘001’ enables the filters  $H(z)$  and  $H(z^{1/2})$  and storage 1, which produces the sub-bands of scheme 1 and the results are stored in storage 1. The scheme 1 also defines the four regions of the audiogram for masking purposes when using higher schemes. The control switch status ‘010’ enables the filters  $H(z)$ ,  $H(z^{1/2})$ ,  $H(z^{4/2})$  and storage 2, and the sub-bands of scheme 2 are stored in storage 2. Similarly, the control switch status ‘100’ enables the filters  $H(z)$ ,  $H(z^{1/2})$ ,  $H(z^{4/2})$ ,  $H(z^{8/2})$  and storage 3, and the sub-bands of scheme 3 are stored in storage 3. The sub-bands in each region are selected from the above storages based on the scheme selection method.

### 3.5 Hardware Implementation

The hardware realization of the proposed reconfigurable filter bank structure is shown in Fig. 4. The prototype filter,  $H(z)$  is an odd length linear phase FIR filter with coefficients  $[h_{(N-1)/2}, \dots, h_1, h_0, h_1, \dots, h_{(N-1)/2}]$ , where  $N$  represents the order of the filter. The transposed form for FIR filter design was used for realization, to share the multipliers for reducing the complexity and device utilization. The  $L$ -fold interpolation operation is realized by replacing each delay element with  $L$  cascaded elements. The decimation by  $D$  operation is done by taking the  $D^{th}$  coefficients only and discarding all others. Since the cascading procedure does not increase the number of coefficient multipliers, the complexity of the interpolated filter is not changed. The complementary pairs of the filters are generated by subtracting the response of respective filters from the original signal. In Fig. 4, a 7-tap prototype filter with coefficients  $[h_3, h_2, h_1, h_0, h_1, h_2, h_3]$  is taken for the realization of the fractional interpolated and complementary filters.

The simulation and verification of the proposed structure are done using Matlab R2017b, and the hardware implementation is performed in Verilog language using Xilinx Vivado 2018.3 on Kintex7 FPGA board. The hardware implementation of the proposed structure is compared with structures in [17, 18] and the results are shown in Table 6. The

**Table 5. Calculation of hearing variations in different regions.**

Region	Frequency range	Slopes
1	0 - 2kHz	$V_1 = \max( d_1 ,  d_2 ,  d_3 )$
2	2kHz - 4kHz	$V_2 =  d_4 $
3	4kHz - 6kHz	$V_3 =  d_5/2 $
4	6kHz - 8kHz	$V_4 =  d_5/2 $

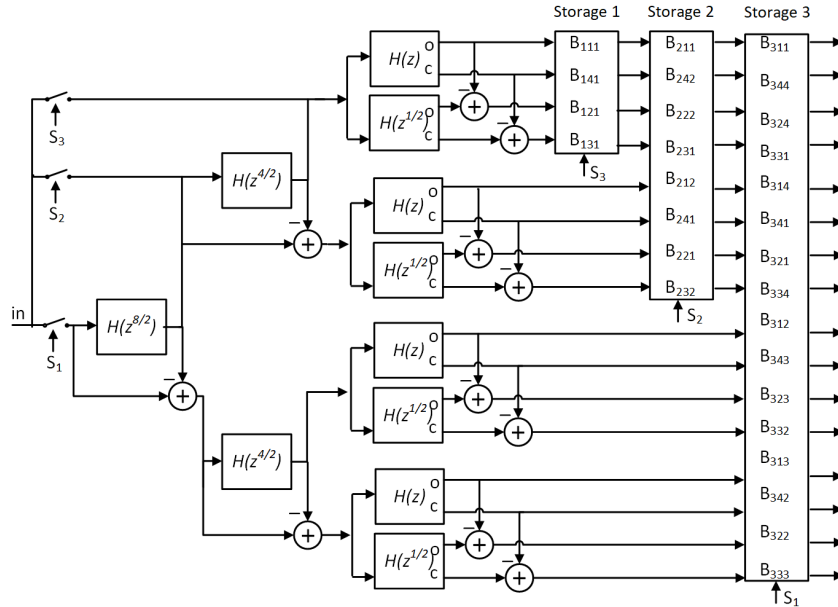


Fig. 3. Structure of the proposed reconfigurable filter bank.

sampling frequency of the audiogram matching process is 16kHz. Table 6 depicts that the device utilization and the power dissipation at 16kHz of the proposed structure are very less compared to other structures. The structure of the proposed reconfigurable filter bank presented in Fig. 3 is easily implemented, as illustrated in Fig. 5. Three dual pole switches are used to toggle between the original and complementary outputs of the filters. Initially, all the toggle switches connect the original low pass outputs of the filters to the following stages. The toggling time of the switches  $T_1$ ,  $T_2$ , and  $T_3$  are 3.18ms, 1.59ms, and 0.79ms respectively, which corresponds to the group delays of the filters  $H(z^{4/2})$ ,  $H(z)$ , and  $H(z^{1/2})$ . The outputs of the filters in every cascaded connection are stored in the storage element.

**Table 6. Device and power utilization.**

Utilization data	Structure in [17]	Structure in [18]	Proposed structure
Number of slice registers	5376	4557	3368
Number of LUTs	13092	11511	9687
Number of FF pairs	4160	3378	2892
Power at 16kHz (Watt)	0.470	0.470	0.414

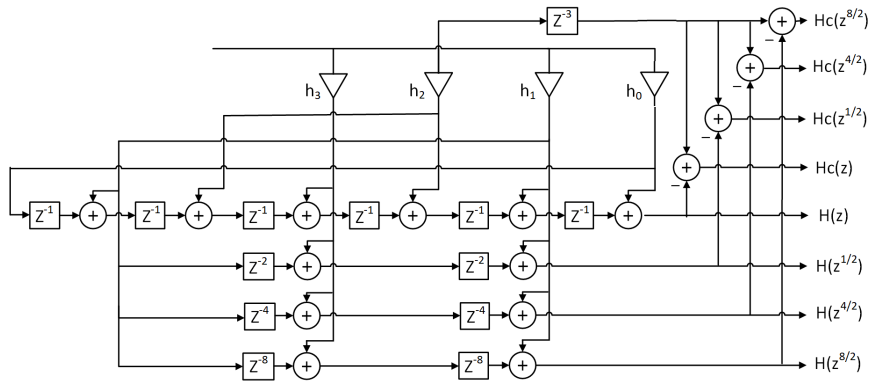


Fig. 4. Proposed hardware realization of the filters.

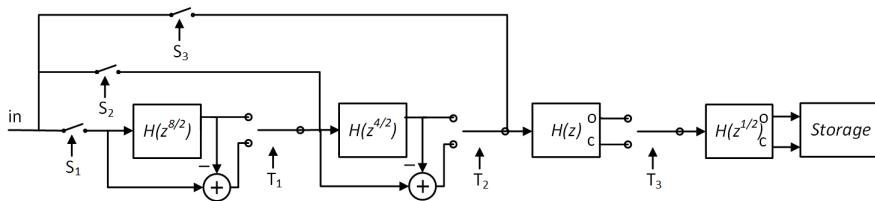


Fig. 5. Proposed hardware realization of the hearing aid.

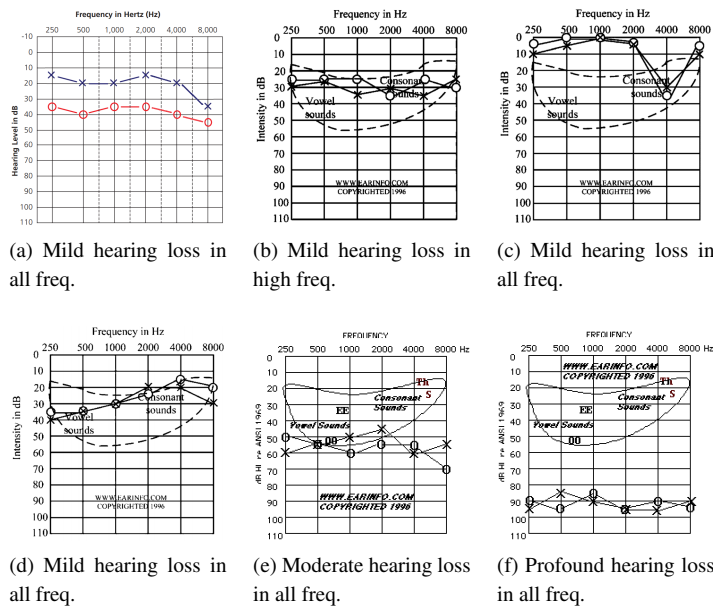


Fig. 6. Audiograms having mild to profound hearing losses.

**Table 7. Scheme selection and corresponding delays in audiogram matching.**

Test audiogram	Region 1	Region 2	Region 3	Region 4	Delay (ms)
Fig.6(a) left ear	Scheme 1	Scheme 1	Scheme 2	Scheme 2	5.56
Fig.6(a) right ear	Scheme 1	Scheme 1	Scheme 1	Scheme 1	2.38
Fig.6(b) left ear	Scheme 2	Scheme 1	Scheme 1	Scheme 1	5.56
Fig.6(b) right ear	Scheme 2	Scheme 2	Scheme 1	Scheme 1	5.56
Fig.6(c) left ear	Scheme 1	Scheme 3	Scheme 2	Scheme 2	11.92
Fig.6(c) right ear	Scheme 1	Scheme 3	Scheme 2	Scheme 2	11.92
Fig.6(d) right ear	Scheme 1	Scheme 2	Scheme 1	Scheme 1	5.56
Fig.6(e) right ear	Scheme 1	Scheme 1	Scheme 2	Scheme 2	5.56
Fig.6(f) left ear	Scheme 2	Scheme 1	Scheme 1	Scheme 1	5.56
Fig.6(f) right ear	Scheme 2	Scheme 1	Scheme 1	Scheme 1	5.56

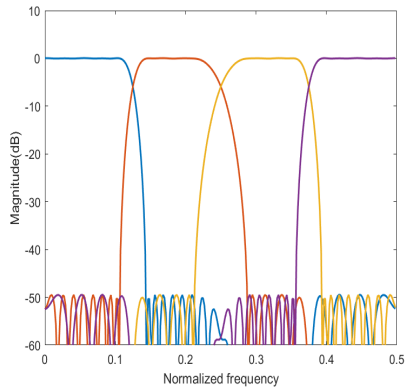
**Table 8. Comparison of matching errors in auditory compensation.**

Test audiogram	Type of hearing loss (HL)	Method in [17]	Proposed method
Fig.6(a) left ear	Mild HL in all frequencies	3.13 dB	2.52 dB
Fig.6(a) right ear	Mild HL in high frequencies	2.83 dB	2.23 dB
Fig.6(b) left ear	Mild HL in all frequencies	2.01 dB	1.98 dB
Fig.6(b) right ear	Mild HL in all frequencies	1.82 dB	1.93 dB
Fig.6(c) left ear	Mild HL in high frequencies	5.27 dB	2.59 dB
Fig.6(c) right ear	Mild HL in high frequencies	5.63 dB	2.71 dB
Fig.6(d) right ear	Mild HL in all frequencies	3.41 dB	2.53 dB
Fig.6(e) right ear	Moderate HL in all frequencies	3.26 dB	2.47 dB
Fig.6(f) left ear	Profound HL in all frequencies	2.16 dB	2.29 dB
Fig.6(f) right ear	Profound HL in all frequencies	2.22 dB	2.15 dB

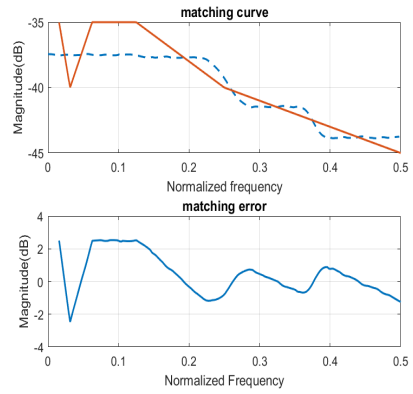
#### 4. PERFORMANCE ANALYSIS

In audiogram matching, the hearing deficiency of a person is restored by adjusting the gains of sub-bands of the filter bank. Various classes of audiograms from mild to profound hearing losses are used for evaluating the performance of the proposed system. In most of the audiograms, the patients suffer from nearly similar losses in both ears called bilateral hearing loss. Audiograms shown in Fig. 6 are taken from the independent hearing aid information, a public service provider of Hearing Allianz of America [27]. The proposed scheme selection method chooses the optimum scheme for compensating the hearing defects shown in different audiograms. The magnitude responses of the corresponding filter banks and their matching results are shown in Fig. 7. The schemes assigned in different regions of the test audiograms and the delays associated with the schemes are listed in Table 7.

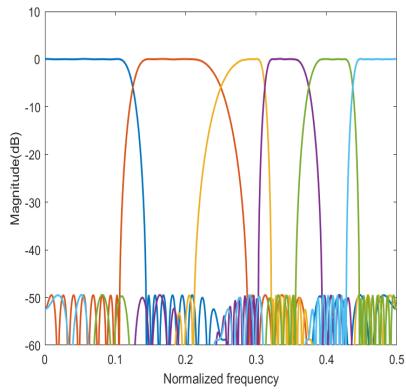
The matching errors are calculated using the proposed reconfigurable structure and compared with an existing method [17], as listed in Table 8. The hearing losses in all the audiograms are compensated effectively within the tolerable limit of  $\pm 3dB$ . From Table 8, it is apparent that the proposed structure delivers better results than existing techniques. Since the hearing aid is a battery-operated device, the complexity is as low



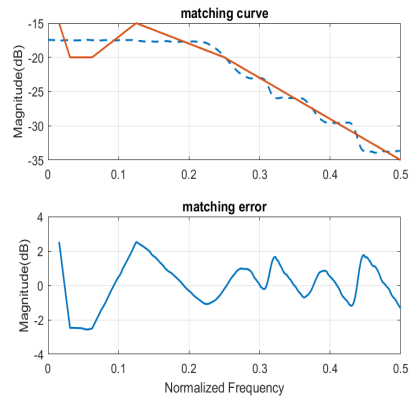
(a) Filter bank response for Fig. 6(a) right ear



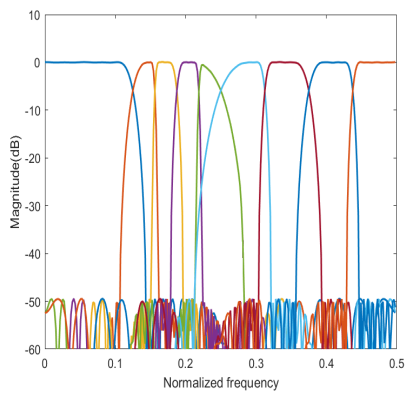
(b) Matching results for Fig. 6(a) right ear



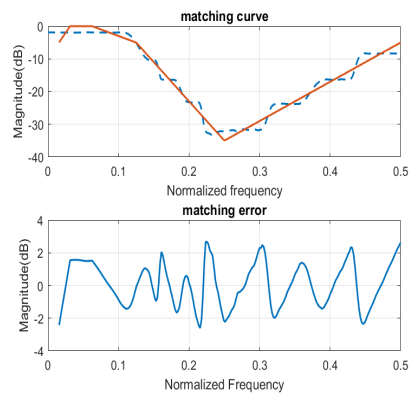
(c) Filter bank response for Fig. 6(a) left ear



(d) Matching results for Fig. 6(a) left ear



(e) Filter bank response for Fig. 6(c) right ear



(f) Matching results for Fig. 6(c) right ear

Fig. 7. Auditory compensation results.

**Table 9. Complexity comparison of the proposed structure with existing methods.**

Method	$f_s$ (kHz)	$\delta_p$ (dB)	$\delta_s$ (dB)	Number of multipliers	Reduction in complexity
ANSI S1.11 [9]	24	1	60	138	81.2%
Quasi-ANSI [10]	24	1	60	226	88.5%
FRM [12]	16	.0001	80	30	13.3%
CMFB [7]	16	.01	110	63	58.7%
VBW Filters [15]	16	.05	80	216	87.9%
MDFT [8]	16	.001	85	84	69%
FI [17]	16	.005	50	76	65.8%
Two-level FI [18]	16	.005	50	67	61.2%
Proposed method	16	.05	50	26	—

**Table 10. Delay comparison of the proposed structure with existing methods.**

Method	Type of filter bank	Number of bands	Maximum delay
ANSI S1.11 [9]	Fixed	18	31ms
Quasi-ANSI [10]	Fixed	18	10ms
FRM [12]	Fixed	8	26.6ms
VBW Filters [15]	Reconfigurable	4 to 10	1.1ms
FI [17]	Reconfigurable	3 to 12	21.6ms
Two-level FI [18]	Reconfigurable	3 to 13	18.5ms
Proposed method	Reconfigurable	4 to 16	11.9ms

as possible to minimize the power consumption and maximize the operating time of the device. The device complexity of the proposed structure is compared with other methods in the literature and listed in Table 9. Since the multiplier is the most power consuming component in the hearing aid, the total number of multipliers used in the design are considered for assessing the complexity of the device. The proposed method is able to achieve a complexity reduction upto 88.5% than other existing techniques. The delay of the proposed structure is compared with existing methods and is shown in Table 10. Fig. 8 gives a graphical comparison between complexity and delay of various methods from which, it is clear that the method proposed in this paper has an optimum value of delay and complexity than other methods. The maximum delay of the proposed structure is only a half of the globally accepted range of 20ms.

## 5. CONCLUSION

A reconfigurable filter bank structure of low complexity for auditory compensation in digital hearing aids is discussed in this paper. The proposed structure is achieved using a single prototype filter with 26 multipliers only. A drastic reduction in multipliers up to 88.5% is obtained in the proposed structure when compared to other similar techniques. The proposed system decomposes the audio spectrum into four regions and three different schemes are suggested in each region. An optimized scheme is selected for each region which is based on the hearing variations in the audiogram. This smart hearing aid is capable of eliminating the numerous trials otherwise required for fixing suitable bands in various frequencies. The same filter bank structure is suited for matching audiograms with

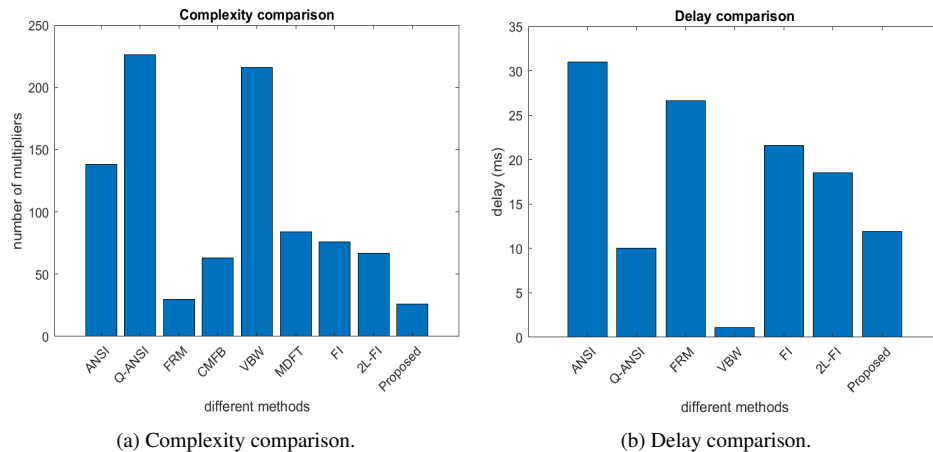


Fig. 8. Comparison of complexity and delay of the proposed structure.

different types of hearing losses, without any modification in the hardware. It is observed that the matching errors and the operational delays are within the tolerable limits. Due to the minimum number of coefficient multipliers deployed in this method, the hardware complexity, power, and chip area required for realization of the structure is minimal, which can be a step towards making the hearing aids cost-effective.

## REFERENCES

1. World Health Organization, <http://www.who.int/news-room/fact-sheets/detail/deafness-and-hearing-loss/>, 2020.
2. T. Devis and M. Manuel, "A low-complexity 3-level filter bank design for effective restoration of audibility in digital hearing aids," *Biomedical Engineering Letters*, Vol. 10, 2020, pp. 593-601.
3. J. Katz, L. Medwetzsky, R. Burkard, L. Hood, *Handbook of Clinical Audiology*, Lippincott, Williams & Wilkins, Philadelphia, PA, 2009.
4. S. Khullar and R. Babbar, "Presbycusis and auditory brainstem responses: A review," *Asian Pacific Journal of Tropical Disease*, Vol. 1, 2011, pp. 150-157.
5. H. Levitt, "Digital hearing aids: A tutorial review," *Journal of Rehabilitation Research and Development*, Vol. 24, 1987, pp. 7-20.
6. C. Schweitzer, "Development of digital hearing aids," *Trends in Amplification*, Vol. 2, 1997, pp. 41-77.
7. S. Kalathil and E. Elias, "Efficient design of non-uniform cosine modulated filter banks for digital hearing aids," *AEU International Journal of Electronics and Communications*, Vol. 69, 2015, pp. 1314-1320.
8. V. Sakthivel and E. Elias, "Design of hardware-efficient digital hearing aids using non-uniform MDFT filter banks," *Signal Image and Video Processing*, Vol. 12, 2018, pp. 1429-1436.

9. Y.-T. Kuo, T.-J. Lin, Y.-T. Li, and C.-W. Liu, "Design and implementation of low-power ANSI S1.11 filter bank for digital hearing aids," *IEEE Transactions on Circuits and Systems-I: Regular Papers*, Vol. 57, 2010, pp. 1684-1696.
10. C. W. Liu, K. C. Chang, M. H. Chuang, and C. H. Lin, "10-ms 18-band quasi-ANSI S1.11 1/3-octave filter bank for digital hearing aids," *IEEE Transactions on Circuits and Systems*, Vol. 60, 2013, pp. 638-649.
11. M. Manuel and E. Elias, "Design of frequency response masking FIR filter in the canonic signed digit space using modified artificial bee colony algorithm," *Engineering Applications of Artificial Intelligence*, Vol. 26, 2013, pp. 660-668.
12. Y. Lian and Y. Wei, "A computationally efficient non-uniform FIR digital filter bank for hearing aid," *IEEE Transactions on Circuits and Systems*, Vol. 52, 2005, pp. 2754-2762.
13. T. B. Deng, "Three-channel variable filter-bank for digital hearing aids," *IET Signal Process*, Vol. 4, 2010, pp. 181-196.
14. J. T. George and E. Elias, "A 16-band reconfigurable hearing aid using variable bandwidth filters," *Global Journal of Researches in Engineering-F: Electrical and Electronics Engineering*, Vol. 14, 2014, pp. 1-7.
15. N. Haridas and E. Elias, "Efficient variable bandwidth filters for digital hearing aid using Farrow structure," *Journal of Advanced Research*, Vol. 7, 2016, pp. 255-262.
16. Y. Wei and D. Liu, "A reconfigurable digital filterbank for hearing-aid systems with a variety of sound wave decomposition plans," *IEEE Transactions on Biomedical Engineering*, Vol. 60, 2013, pp. 1628-1635.
17. Y. Wei and Y. Wang, "Design of low complexity adjustable filter bank for personalized hearing aid solutions," *IEEE Transactions on Audio, Speech, and Language Processing*, Vol. 23, 2015, pp. 923-931.
18. A. Amir, T. S. Bindiya, and E. Elias, "Design and implementation of reconfigurable filter bank for low complexity hearing aids using 2-level sound wave decomposition," *Biomedical Signal Processing and Control*, Vol. 43, 2018, pp. 96-109.
19. T. Devis and M. Manuel, "A 17-band non-uniform interpolated FIR filter bank for digital hearing aid," in *Proceedings of IEEE International Conference on Communication and Signal Processing*, 2018, pp. 452-456.
20. P. P. Vaidyanathan, *Multirate Systems and Filter Banks*, Prentice Hall, NJ, 1993.
21. J. H. McClellan, T. W. Parks, and L. R. Rabiner, "A computer program for designing optimum FIR linear phase digital filters," *IEEE Transactions on Audio and Electroacoustics*, Vol. AU-21, 1973, pp. 506-526.
22. Y. Neuvo, D. Cheng-Yu, and S. K. Mitra, "Interpolated finite impulse response filters," *Transactions on Acoustics, Speech, and Signal Processing*, Vol. 32, 1984, pp. 563-570.
23. R. Lyons, "Interpolated narrowband lowpass FIR filters," *IEEE Signal Processing Magazine*, Vol. 20, 2003, pp. 50-57.
24. A. Mehrnia and J. A. Willson, "On optimal IFIR filter design," in *Proceedings of IEEE International Symposium on Circuits and Systems*, Vol. 3, 2004, pp. 133-136.
25. M. A. Stone and B. C. J. Moore, "Tolerable hearing-aid delays. III. Effects on speech production and perception of across-frequency variation in delay," *Ear and Hearing*, Vol. 24, 2003, pp. 175-183.

26. D. A. Vogel, P. A. McCarthy, G. W. Bratt, and C. Brewer, "The clinical audiogram – Its history and current use," *Communicative Disorders Review*, Vol. 1, 2007, pp. 81-94.
27. "Consumer resource for hearing aids," <http://www.earinfo.com/how-to-read-a-hearing-aid-test/>, 2020.



**Tomson Devis** received B.Tech degree in Electronics and Communication Engineering from Mahatma Gandhi University in 2004 and M.Tech degree from Kerala University in 2006. He is currently pursuing the Ph.D. degree in the Department of Electronics and Communication Engineering at Rajiv Gandhi Institute of Technology, Kottayam, India. His research interests include biomedical image and signal processing, multirate systems, digital filter design, *etc.*



**Manju Manuel** received B.Tech degree in Electronics Engineering and M.Tech degree in Digital Electronics from Cochin University in 1995 and 2001 respectively. She completed the Ph.D. degree in Signal Processing from National Institute of Technology, Calicut, India in 2012. She is working as an Associate Professor in the Department of Electronics and Communication Engineering at Rajiv Gandhi Institute of Technology, India. Her research interests include signal and image processing, multirate systems, digital filter design, *etc.*